ELSEVIER

Journal of Chromatography A, 719 (1996) 275–289

JOURNAL OF CHROMATOGRAPHY A

Consolidation of the packing material in chromatographic columns under dynamic axial compression II. Consolidation and breakage of several packing materials

Matilal Sarker[a,b], Anita M. Katti[c], Georges Guiochon[a,b,*]

[a]*Department of Chemistry, University of Tennessee, Knoxville, TN 37996-1600, USA*
[b]*Division of Chemical and Analytical Sciences, Oak Ridge National Laboratory, Oak Ridge, TN 37831-6120, USA*
[c]*Mallinckrodt Chemical Inc., St. Louis, MO 63147, USA*

First received 12 April 1995; revised manuscript received 3 July 1995; accepted 5 July 1995

Abstract

The consolidation of packing materials under dynamic axial compression is studied for one irregular and two spherical shaped particles. When the total axial compression stress is raised from 1 to 80 kg/cm^2, a long column of initial length 25 cm shrinks by nearly 25%, while a short column of initial length 4 cm decreases by nearly 35%. This result illustrates the lack of homogeneity of the stress distribution during the compression. While the extent of consolidation is nearly the same with all three materials, its kinetics is different. The spherical materials consolidate rapidly and smoothly. The material made of irregular-shaped particles consolidates more slowly, in several decreasing steps. Finally, almost no breakage is observed with the spherical materials, while for the irregular-shaped material fragmentation and chipping takes place to a significant extent under an axial compression stress of 80 kg/cm^2.

1. Introduction

The improvement of the packing methods of columns, whether for gas or liquid chromatography, has been hindered by a lack of understanding of the phenomena which take place during the formation of the bed. For as long as columns have been packed, a purely empirical approach has been used, without any serious reflection being conducted on the basic mechanics and physics of packing. No attention has yet been paid to the possibility that the packing density could depend on the experimental conditions of the packing process. However, consolidation of powders is as common to our daily experience as a footprint in wet sand.

Any particulate material submitted to stress consolidates. The phenomenon is absolutely general. It is observed, studied and used in soil mechanics [1–4], ceramics, powder metallurgy, the storage of pulverulent materials such as concrete or flour [5], and in the manufacturing of tablets [6–8]. The methodology developed, the procedures used for the study of soil properties,

* Corresponding author. Address for correspondence: Department of Chemistry, University of Tennessee, 575 Buehler Hall, Knoxville, TN 37996-1600, USA.

0021-9673/96/$15.00
SSDI 0021-9673(95)00750-4

and the results obtained in soil mechanics are the most useful for our purpose to investigate the behavior of packing materials in chromatographic columns [1–4]. The stress applied to the material during its consolidation in powder metallurgy is very high and the integrity of the powder particles is not preserved. A dense, solid part is obtained. The experimental conditions are too remote from those achieved during the packing of chromatographic columns for these studies to be useful for our purpose. The same is true, albeit to a lesser extent for the study of the manufacturing of the green bodies in ceramics or of tablets in the pharmaceutical industry [6–8]. In the former case, retention of the mold shape is of primary concern. In the latter case, the particles of the original material lose their integrity. However, there is a great similarity between the first stage of the compression of solid powders to make a tablet and the compression of packing material in an axial compression column. The results obtained by Train [6–8] are highly relevant to our general purpose. Finally, the stress experienced by powders during their storage in large-size silos is moderate compared to the stress experienced during the consolidation of columns [5].

In a previous paper [9], we reviewed the pertinent literature on the consolidation of soils and the concepts relevant to the behavior of fine particulate materials, such as sands and silts. Note that the most popular packing materials used in high-performance liquid chromatography have the dimensions of medium silts (5 to 20 μm), while some materials used in large-size preparative columns could be considered as coarse silts (20 to 60 μm) [4]. We discussed the application of these concepts to the silica-based packing materials used in chromatography and showed that the consolidation kinetics of a conventional packing material presents some unusual peculiarities which makes it different from that of soils, the consolidation proceeding slowly, by jumps to metastable states. In this preliminary study, the consolidation of a relatively long bed (ca. 20–25 cm) was investigated. The samples studied in soil mechanics are wider than high, which limits the influence of the wall friction on the consolidation of the sample.

The goal of this paper is the discussion of the development of a systematic methodology of testing packing materials used in chromatography for their behavior during their consolidation. The successful operation of industrial preparative chromatography requires that the column be stable and its characteristics constant. The demonstration of bed stability and reproducibility of the chromatographic operation is necessary to proving control of the process as required by current Good Manufacturing Practice (cGMP). The achievement of a stable column requires its complete consolidation. The time required to consolidate depends on the material used and possibly on the column length and diameter. On the other hand, it would be useful to be able to control the degree of consolidation. The column permeability decreases with decreasing external porosity, hence, with increasing extent of consolidation. This study provides a deeper understanding of the consolidation process.

2. Experimental

2.1. Equipment

A dynamic axial compression skid LC.50.VE.500.100 (Prochrom, Champigneulles, France) with a 59×5.0 cm I.D. stainless steel column was used. The piston is actuated by a hydraulic jack, itself driven by an air compression pump from Haskel (Burbank, CA, USA). A compression pressure adjustable up to 100 kg/cm^2 may be applied to the packing material contained in the column. The column walls are polished, with an RA (arithmetic mean roughness value) between 0.2 and 0.4 μm. A series of chevron seals prevents leaking between the piston and the wall of the column. Most compression experiments are made without flow of mobile phase through the column, except for the slurry solvent which is free to flow out of the column through the normal exit, in the top flange. In these experiments, the column inlet (piston side) is kept closed.

In some experiments, a steady stream of mobile phase is pumped through the column

using a Kiloprep 100 HPLC pump from Biotage (Charlottesville, VA, USA). The pump can deliver solvent at a maximum flow-rate of 500 ml/min and a maximum pressure of 138 kg/cm^2. The flow-rate is set manually. The system includes an injection valve with a 1.5-ml injection loop.

2.2. Packing material

Three octadecyl bonded silica packing materials were used. Two of these materials are made of spherical particles, having an average particle size of approximately 10 and 20 μm, respectively. The third is made of irregular-shaped particles with an average particle size of 20 μm. All have an average pore size of 100 Å. The names under which they are referred to in this work and their main characteristics are reported in Table 1. The material was dried, weighed and slurried in isopropanol, following conventional procedures [10].

2.3. Procedures

In all cases, for the entire duration of each experiment, the column length was monitored using the position sensor fixed to the piston as previously described [10]. The range of this sensor is approximately 0.8 cm, while the changes observed in the length of the column are typically several cm (up to 6). Thus, several adjustments in the sensor position are required during most experiments.

Compression

The slurry is poured into the column and left to decant for several hours. The supernatant is collected with a large syringe, then, the top flange is closed and a 1 kg/cm^2 compression stress is applied. The solvent expelled during the consolidation is collected in a graduated cylinder. The initial column length is measured [11], the compression stress is increased stepwise, and the variations of the column length recorded. The whole compression process takes place while the particles are in contact with pure isopropanol. Although the nature of the solvent is obviously a parameter of importance in the consolidation of the slurry, it has not yet been investigated. After the maximum compression pressure is reached, the column is washed with fresh methanol, equilibrated in closed circuit for several hours, and its final length is measured.

Decompression

The design of the equipment does not permit progressive decrease of the compression pressure. The leak in the hydraulic system is too small when closed, too large when open. The procedure adopted consists in decompressing the column, then, recompressing it rapidly at the lower pressure selected.

Measurements of column efficiency and permeability

As explained above, the consolidation of the column under increasing compression stress is carried out stepwise. Several times during this operation, a stream of mobile phase is pumped through the column at increasing set flow veloci-

Table 1
Characteristics of the materials used

Name	Shape	$\bar{d}_p$[a] (μm)	$\bar{\pi}$[b] (Å)	P_M[c] (atm)	M/V[d] (g/cm^3)
A	Irregular	20	100	66	0.611
B	Spherical	13	100	92	0.606
C	Spherical	10	150	94	0.749

[a] Average particle size.
[b] Average pore size.
[c] Maximum stress experienced.
[d] Apparent consolidation density, under P_M.

ties, the head pressure and the column efficiency for small size samples are measured. During these experiments, the compression stress applied to the piston is kept constant. Hence the effective stress applied to the bed decreases by the amount corresponding to the value of the head pressure (see below, Discussion).

Particle size distribution

When the consolidation experiments were finished, the top flange was unfastened and the packing extruded from the column by raising the piston. The column bed was extruded in one piece. Although brittle, it can be taken in the hand, carried to the bench, and examined. Radial or axial cross-sections can be made with a knife. Samples of the packing material were collected in different locations, in the center and along the wall, near the top flange, in the middle of the column, near the piston and against the piston frit (eight samples). These fractions were submitted to analysis of their particle size distribution and scanning electron microscopic pictures of selected samples were recorded. The measurements of the particle size distribution were made with a Coulter counter on samples of virgin material and on the samples collected in the column bed as just explained.

Scanning electron micrography

A small portion of each sample of the packing materials was deposited onto adhesive on aluminum SEM stubs and densely distributed across the stub. Each specimen was sputter-coated with Au/Pd alloy to impart electrical conductivity. The specimen was examined with the secondary electron detector in the SEM, looking at a fairly wide area of the specimen surface. Two regions which appeared to best typify the particles observed were photographed at 500 × magnification. A part of each region selected to include details of an anomalous particle was recorded at magnification 2500 × .

3. Results and discussion

Experiments were performed first on relatively long columns, typical of those used in preparative chromatography, then on much shorter columns, which have lengths typical of the thickness of soil samples tested for soil performance [1].

3.1. Compression of chromatographic columns

A typical plot of the column length during a compression step of the irregular-shaped particles (A) is shown in Fig. 1. This figure shows the decrease in column length as a function of time after the compression stress has been raised from 29.3 to 41.8 kg/cm^2. This consolidation curve confirms previous results obtained in the compression of a different column prepared with the same packing material [9]. With material A, the consolidation equilibrium is not reached continuously, in a progressive adjustment of the position of the diverse particles but by a successions of jumps, through metastable states. This makes the experiments more complex, as it is not easy to recognize that final consolidation has been reached and when the eventual equilibrium is achieved. For this reason, the actual duration of the consolidation experiments is much longer than actually shown in the figures.

As noted in a previous publication, there are three successive steps in the consolidation of a column prepared from a slurry [9]. These steps

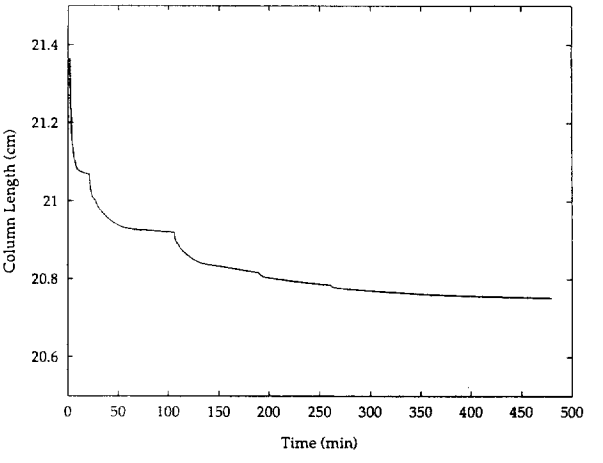

Fig. 1. Kinetics of consolidation under axial compression stress of a packing material; 238 g of irregular-shaped particles (material A, Table 1); compression stress raised abruptly from 29.3 to 41.8 kg/cm^2.

are also encountered in the compression of loose sands or silts [1,4] and in the early stages of tablet compression [6,7]. First, the particles are brought into close contact. Contact forces develop between adjacent particles, at the contact points. Local stresses are very high. As a result the particles deform in an elastic or plastic strain around the contact points. In a second step, the shear forces between particles cause them to slide. This sliding and the subsequent rearrangement of the particle skeleton [9] accounts for most of the strain. Eventually, at high stress levels, a large number of particles begin to break and merge. Except for its onset, this last step is outside the range of our concern. Note that particles, especially those of irregular shape, may begin to chip early in the second stage. The phenomenon of jumps through a series of metastable positions, reported previously [9] and observed in Fig. 1, has not been described in soil consolidation. It does not seem to take place during the first phase of consolidation, at relatively low compression stresses (i.e., below ca. 20 kg/cm^2). At least, we never observed it to take place except at relatively high stresses, in the second step. We suggest that it results from the wedging of shear movements by the asperities of some particles placed at strategic locations. Considerable stress accumulates on the keystone particles which eventually chip or break, releasing stress in a local particle slide. These events are too few, however, to have any significant consequences on phenomena of direct interest in chromatography. They may explain, however, why it may take a certain time (several hours to a few days with widebore columns) before a new column bed becomes dimensionally stable.

A confirmation of this interpretation is given by the plots of the column length versus time during the consolidation under stress of the spherical particles of material B, illustrated in Fig. 2. Neither in Fig. 2a (low compression stress) nor in Fig. 2b (high compression stress) can we see any abrupt jump of the column length with the first spherical-particles material. However, with the second spherical material, C, the same phenomenon of a succession of metastable states during consolidation is noticed, as shown in Fig. 3 (medium compression stress, zone 2). This results in a much longer process. As a matter of fact, it is not sure that this process is ever completed. The consolidation curves observed at low compression stress or at any stress for the spherical material B are very similar to those observed for fine sands and silts and reported in the literature [1,4]. The rate of consolidation is high, 95% of the strain is

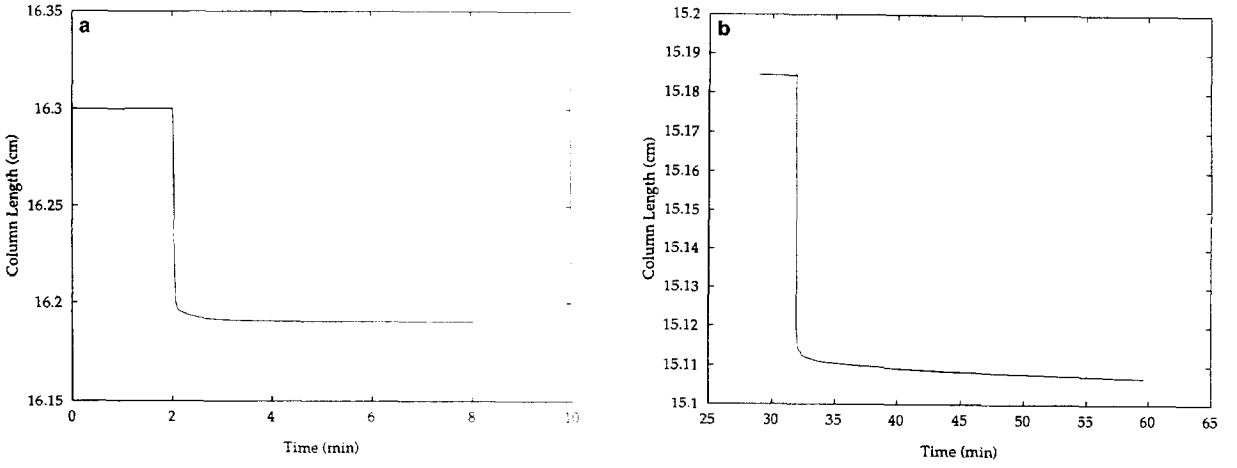

Fig. 2. Kinetics of consolidation under axial compression stress of a packing material; 180 g of spherical particles (material B, Table 1); (a) compression stress raised abruptly from 10.5 to 14.6 kg/cm^2; (b) compression stress raised abruptly from 81.8 to 92.0 kg/cm^2.

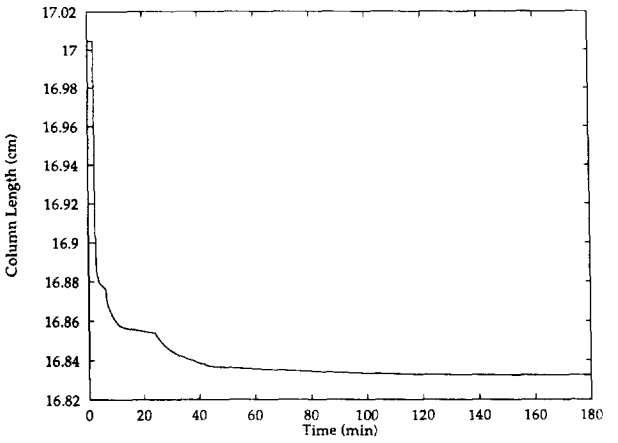

Fig. 3. Kinetics of consolidation under axial compression stress of a packing material; 238 g of spherical particles (material C, Table 1); compression stress raised abruptly from 25.1 to 37.6 kg/cm^2.

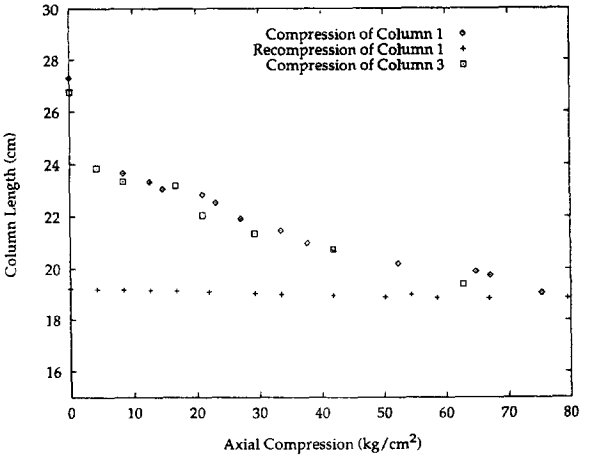

Fig. 4. Length of the consolidated column after equilibrium is reached as a function of the compression stress; 238 g of irregular-shaped particles (material A).

achieved in the first minute, 99% in less than 10 min *. The difference in behavior of the materials B and C is probably explained by the difference in the aspect of their particles.

A plot of the length of the consolidated column after equilibrium has been reached as a function of the compression stress is given in Fig. 4 for the irregular-shaped particles of material A and in Figs. 5 and 6 for the two materials made of spherical particles, B and C, respectively. Fig. 4 contains data for the compression of two columns containing the same weight of the same material and illustrates the reproducibility of the experiment, in spite of the difficulties encountered in deciding that equilibrium has been reached. This figure shows also the consolidation curve obtained by decompressing the column and recompressing it without perturbing the packed bed. The rebound of the packing upon decompression is small, of the order of 1 to 1.5%. Recompression brings the column back to the same density it had when compression was stopped. The particles do not slide back to their initial position. They cannot; there is no mechanism for this. The sliding movements are irreversible. So, the extent of the rebound is the result of the elastic compression of the particles and is quite limited.

In the case of spherical particles, a smaller amount of material was used for the fist column (B) than for the other two (A, in Fig. 3 and C, in Fig. 5) and this column was initially shorter. The

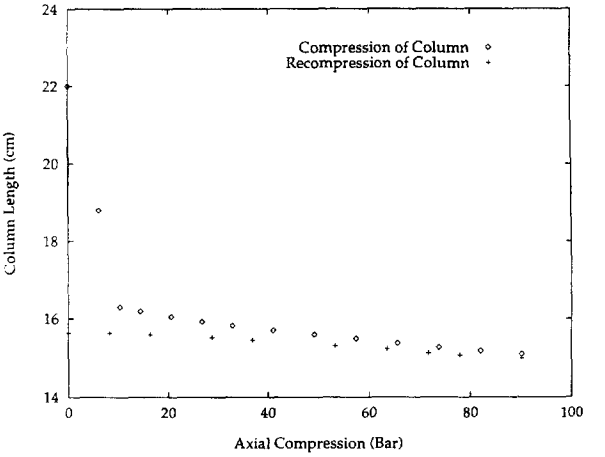

Fig. 5. Length of the consolidated column after equilibrium is reached as a function of the compression stress; 180 g of spherical particles (material B).

* This time is considerably shorter than the settling times (typically years) encountered in soil mechanics. The reason for the slow settling of buildings originates in the large size of the masses of soil involved, their low permeability and the long time needed for the expulsion of the water which is required for the equilibrium strain to be achieved. This is not a problem under the experimental conditions of preparative chromatography.

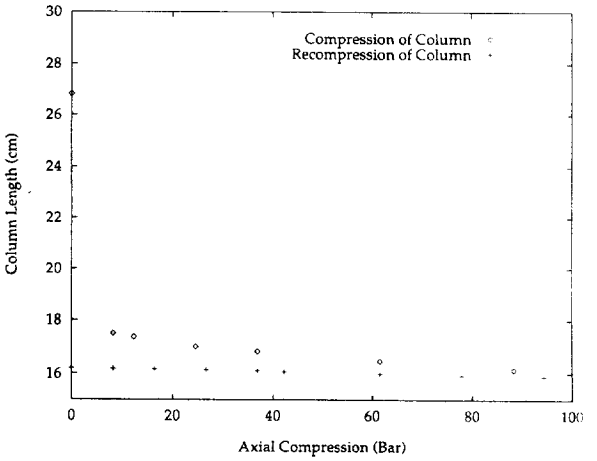

Fig. 6. Length of the consolidated column after equilibrium is reached as a function of the compression stress; 238 g of spherical particles (material C).

difference in the lengths of the consolidated columns packed with materials A and C or in the ratio of the mass of packing to the length of the consolidated column (Table 1) can be ascribed to the difference in the porosity of the materials used. However, the relative decrease in column length, hence in packing volume is approximately the same, one fourth. Note that the relative increase in packing density is also approximately 25%. The decrease in external porosity is larger, as discussed later. The distance between the compression and decompression curves in Figs. 5 and 6 is much less than in Fig. 4. The compression of irregular-shaped particles is more progressive and requires higher levels of stress. Most of the extent of consolidation of the spherical particles under compression is achieved for a stress of 10 kg/cm^2. The same result requires nearly 70 kg/cm^2 for irregular-shaped particles.

Finally, the recompression curves suggest that dynamic compression might not be necessary. Axial compression permits the rapid achievement of a high degree of packing consolidation. Once achieved, there is no mechanism for a return to the previously less dense packing. Further measurements, described later, confirm this result. We have shown elsewhere [10] that voids can be formed at the column inlet by withdrawing the piston, thus causing a major efficiency loss, and that they can be sealed by pushing the piston back in place against the bed, in the process restoring entirely the initial column efficiency. So, as long as consolidation is achieved under a sufficient compression stress, which has to be markedly higher than the stress under which the column is operated, and the piston is not withdrawn, it does not seem necessary to apply permanently a high compression stress to the column packing.

3.2. Compression of short columns

The technical literature on soil mechanics and on the fabrication of tablets by compression of dry powders in a dye suggests that friction along the wall is an important factor in the consolidation of powders under axial stress [6,7]. Therefore, we also studied the compression of much shorter columns obtained by using approximately eight times less packing material than in the previous study. The results regarding the kinetics of consolidation are illustrated in Fig. 7 for the first spherical-particles material (B) and in Fig. 8 for the irregular-shaped particles (A). The metastable states are clearly seen in the latter case, although the importance of the phenomenon is considerably reduced compared to that of the long columns (compare Figs. 1 and 7).

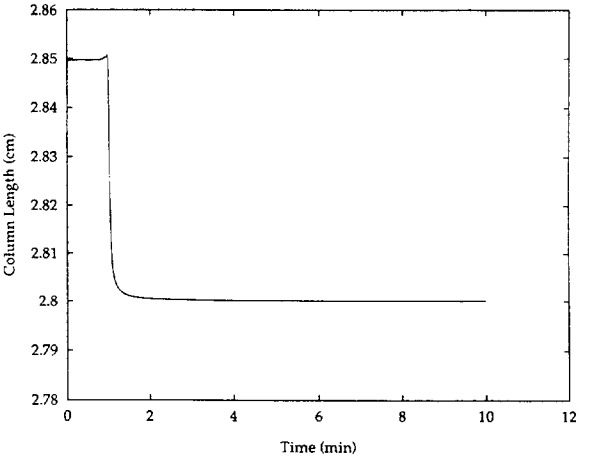

Fig. 7. Kinetics of consolidation under axial compression stress of a packing material; 30 g of spherical particles (material B); compression stress raised abruptly from 41.8 to 62.7 kg/cm^2.

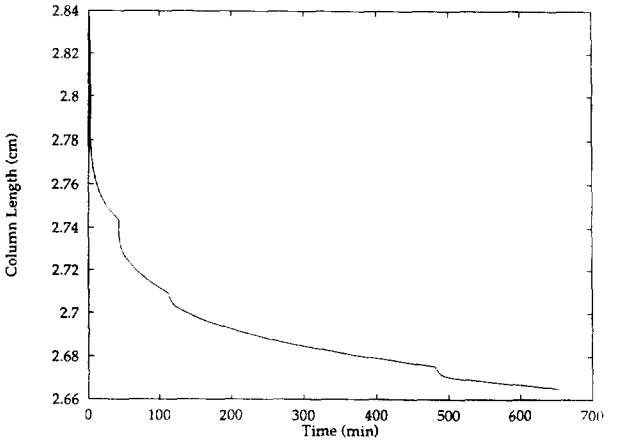

Fig. 8. Kinetics of consolidation under axial compression stress of a packing material; 31 g of irregular-shaped particles (material A); compression stress raised abruptly from 41.8 to 62.7 kg/cm^2.

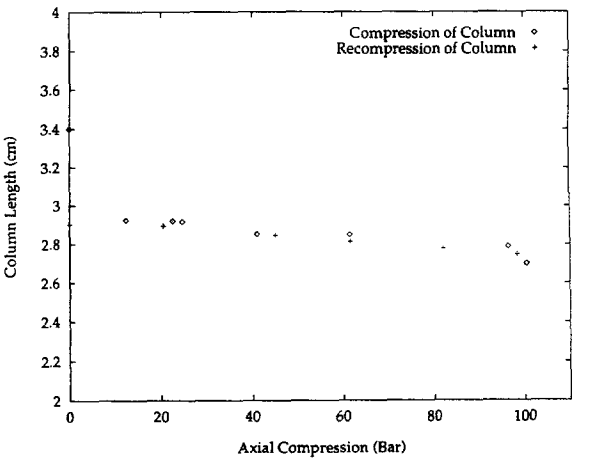

Fig. 10. Length of the consolidated column after equilibrium is reached as a function of the compression stress; 30 g of spherical particles (material B).

The plot of the length of these consolidated columns versus the compression stress are given in Figs. 9–11 for the irregular-shaped (A, Fig. 9) and the two spherical-particles materials (B, Fig. 10 and C, Fig. 11). The behavior of the extent of consolidation of the irregular-shaped material as a function of the compression stress is similar in the long and short columns. However the relative loss of length, i.e. the increase in packing density, tends to be higher with the short columns.

3.3. Influence of the compression stress on the column permeability

Experiments were carried out on several of the columns at different steps of their compression. The permeability was measured as the slope of the plots of the mobile phase flow-rate versus the

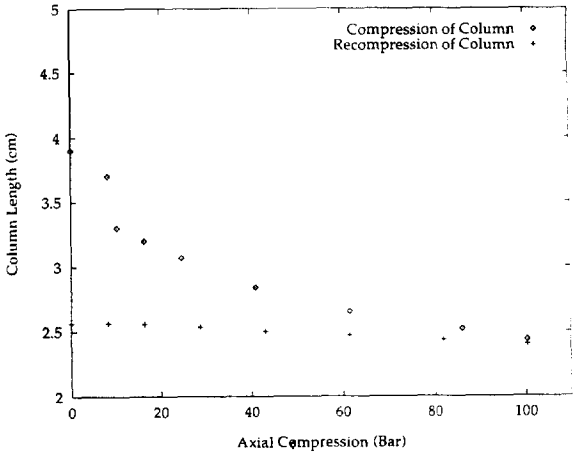

Fig. 9. Length of the consolidated column after equilibrium is reached as a function of the compression stress; 31 g of irregular-shaped particles (material A).

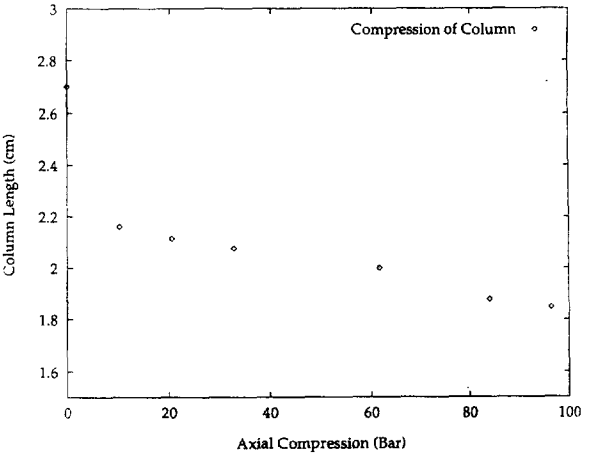

Fig. 11. Length of the consolidated column after equilibrium is reached as a function of the compression stress; 30 g of spherical particles (material C).

Table 2
Permeability of consolidated columns[a]

ACP (kg/cm^2)	ϵ_T	F	Apparent d_p	ΔP (kg/cm^2)
12.5	0.68	0.47	10.11 ± 0.14	4.9
37.6	0.66	0.50	9.17 ± 0.14	5.7
62.7	0.66	0.50	8.53 ± 0.20	6.4
92.0	0.65	0.53	8.01 ± 0.12	7.1

[a] Spherical packing material C.
ACP: axial compression pressure; ϵ_T: total porosity of the bed; F: phase ratio, $F = (1 - \epsilon_T)/(\epsilon_T)$; ΔP: inlet pressure required for a water flow velocity of 0.1 cm/s (equivalent to ca. 1.4 ml/min in an analytical column) through a 17.5 cm long column.

column inlet pressure. Data are reported in Table 2 for the column packed with the spherical material C. The permeability decreases with increasing compression stress. This observation is confirmed by a compilation of apparent average particle sizes calculated assuming a constant external porosity (Table 3). As a consequence, if the classical relationship between the permeability and the average particle size is applied, the particle size appears to decrease. In fact, this would be the wrong interpretation. The correct one is as follows. The particle size remains constant because the elasticity of silica particles is negligible in the stress range involved, as a first approximation. However, under stress the packing density increases and the external porosity decreases. The Blake–Kozeny equation provides a relationship between these parameters

$$k = \frac{d_p^2 \epsilon_e^3}{h_0(\epsilon_i + \epsilon_e)(1 - \epsilon_e)^2} \quad (1)$$

where k is the column permeability, d_p is the average particle diameter, ϵ_e is the external porosity of the column (or volume fraction of the column occupied by the stream of mobile phase percolating around the particles), ϵ_i is the internal porosity of the packing (or volume fraction of the column occupied by the stagnant mobile phase, inside the particles), and h_0 is a geometrical constant, usually of the order of 180, but which can vary from one packing material to the next and is probably somewhat smaller for spherical particles than for irregular ones. The column permeability is derived from experimental data through

$$k = \frac{u\eta L}{\Delta P} \quad (2)$$

where u is the mobile phase velocity, η its viscosity, L the column length, and ΔP the head pressure.

These results permit an independent estimate

Table 3
Apparent particle size

Method	Conditions	Stress[a] (kg/cm^2)	Irregular	Spherical
Coulter counter	RCC	28.8	20.5 ± 0.20	
	ACC	62.7	20.0 ± 0.4	
		63.2		11.5 ± 0.5
		79.4	21.4 ± 0.99	
		92.0		11.19 ± 0.01
Permeability	RCC	5.3	24.6 ± 0.6	
		7.0	21.2 ± 0.6	
		21.1	16.9 ± 0.2	
	ACC	41.8	19.0 ± 0.5	
		63.2	12.3 ± 0.3	
		91.8	9.6 ± 0.3	

[a] Maximum stress applied to the packed bed during the whole series of experiments performed prior to the measurement of the permeability.
RCC: radial compression column; ACC: axial compression column.

of the variation of the external porosity during the column consolidation. This in turn allows the calculation of the void ratio, e, or ratio of the volume available to the flowing mobile phase and the total volume occupied by the particles, so

$$e = \frac{\epsilon_e}{1 - \epsilon_e} \tag{3}$$

The void ratio is the parameter used conventionally in soil mechanics for the interpretation of consolidation data [9]. It is more difficult to measure in chromatography than in soil mechanics because the particles are porous in the former case. This problem will be discussed in a further publication [12].

3.4. Variation of the column efficiency during consolidation

We measured the column efficiency as a function of the mobile phase velocity for columns at different degrees of consolidation. We have not been able to achieve an efficiency comparable to the one obtained with the same packing material when the column was packed following the conventional procedure [11]. It seems that slow consolidation is not compatible with the achievement of a good column efficiency. Much better efficiencies, with values of the reduced plate height of 2.5, have been obtained by achieving fast consolidation under moderate compression stress [10,11]. Thus, it is arguable whether the results of these new HETP (height equivalent of a theoretical plate) measurements are meaningful. For the time being, we merely report the results obtained with one of the spherical particle materials (packing material C). Four HETP versus flow-velocity curves are plotted in Fig. 12. They were obtained with the same column for compression stresses of 12.5, 37.6, 62.7, and 92.0 kg/cm^2, respectively. The maximum value of the column efficiency does not improve with increasing compression stress but tends to decrease slowly as well as the coefficient which accounts for the contribution of the mass transfer resistances. The best values of the coefficients of a Van Deemter equation are reported in Table 4.

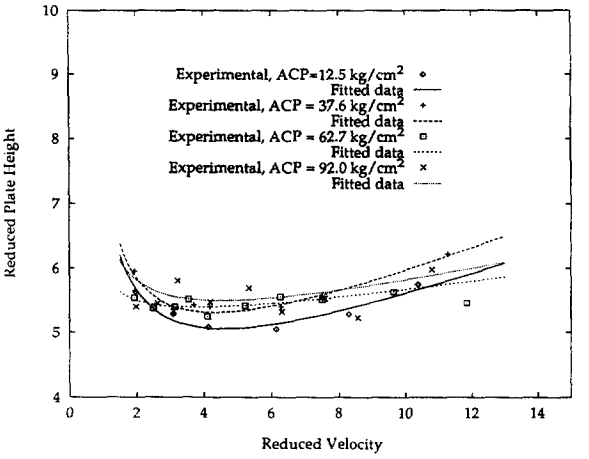

Fig. 12. HETP of the column prepared with 238 g of spherical particles (material C) after consolidation under different compression stress. (◇) 12.5 kg/cm^2; (+) 37.6 kg/cm^2; (□) 62.7 kg/cm^2; (×) 92.0 kg/cm^2. Best coefficients of a Van Deemter equation in Table 4.

Given the scatter of the experimental points, it does not seem that the four curves are significantly different.

3.5. Particle breakage

The particles in the samples collected from different locations in the column bed, at the time when the column was emptied, were studied by electron photomicrography and determination of their particle size distribution, as described in the Experimental section.

Irregular-shaped material

The photomicrographs in Figs. 13–15 illustrate the particle shape and size distribution of the irregular-shaped particles, A. The virgin irregular-shaped material (Fig. 13) on the one

Table 4
Parameters of the Van Deemter plots obtained at different axial compression stress

ACP	a	b	c
12.5	3.4	3.8	0.19
37.6	3.6	3.8	0.20
62.7	4.8	1.0	0.072
92.0	4.5	2.1	0.107

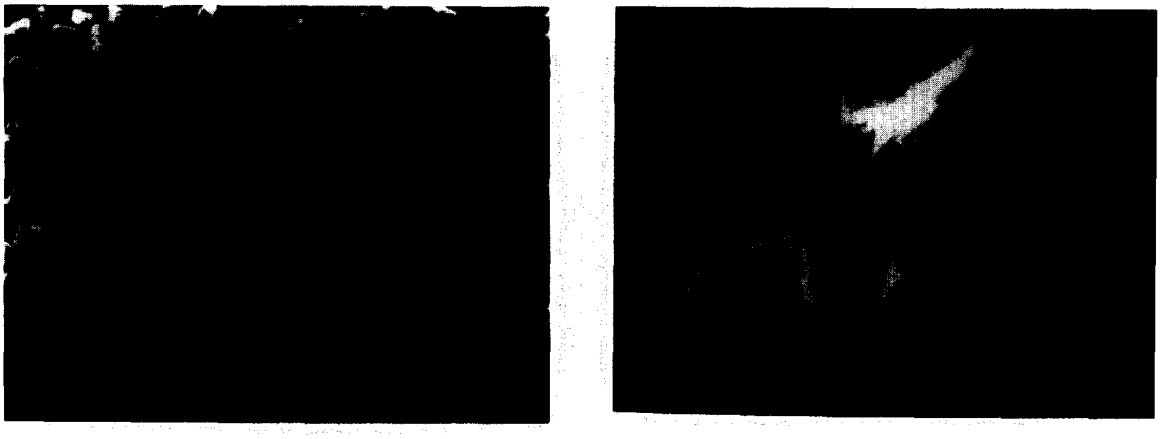

Fig. 13. Photomicrographs of the virgin irregular-shaped particles (material A). Magnification: (a) 125 × ; (b) 1250 × .

hand, and any material recovered from compression studies on the other hand (Figs. 14 and 15) have very different aspect. Evidence of chipping and/or minor fragmentation in the material recovered from close-to-the-piston frit (Fig. 14) or close to the wall, at the top of the column (Fig. 15) is clear. There is a large number of small particles sticking to the larger ones clearly visible on Fig. 15b. The extent of the fragmentation observed seems to be limited, however, to the abrasion of sharp edges and there appears to be only few large particles broken.

The extent of the fragmentation is sufficient, however, to affect the volume size distribution statistics in the cases when a high compression stress is achieved. Fig. 16 shows the volume size distribution of the particles contained in four samples. Samples 1 and 2 come from the dry compression experiment and samples 3 and 4 from the first wet compression experiment described in a previous report [9]. Samples 1 and 3 were taken from the center of the packing, right against the piston frit. Samples 2 and 4 were taken from the packing against the wall, at the bottom of the bed, close to the piston. Only sample 1 has suffered enough abrasion to exhibit an important change in its particle size distribution. Fine particles have been formed in significant proportion while for the other three samples the low size part of the distribution is identical to

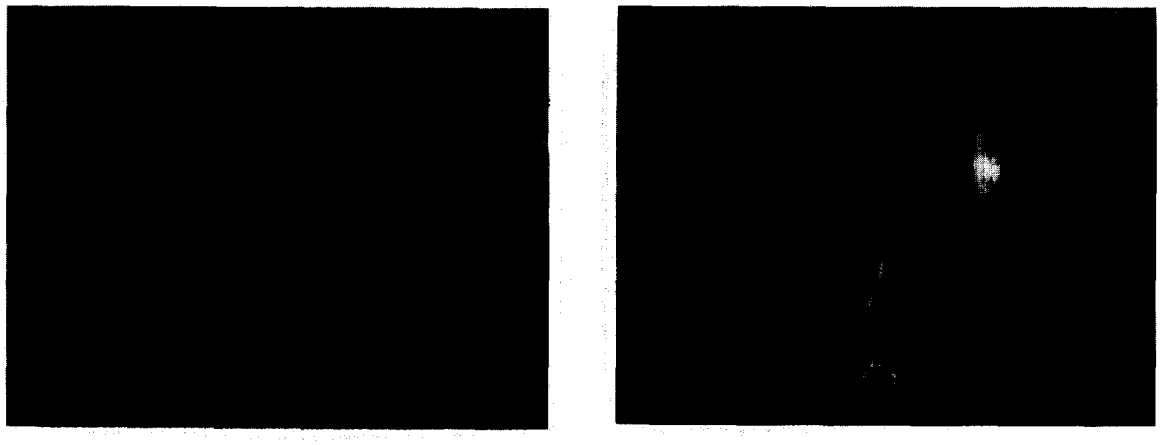

Fig. 14. Photomicrograph of a sample of the irregular-shaped particles (material A) taken from the part in direct contact with the piston frit, in the center of the column. Magnification: (a) 125 × ; (b) 1250 × .

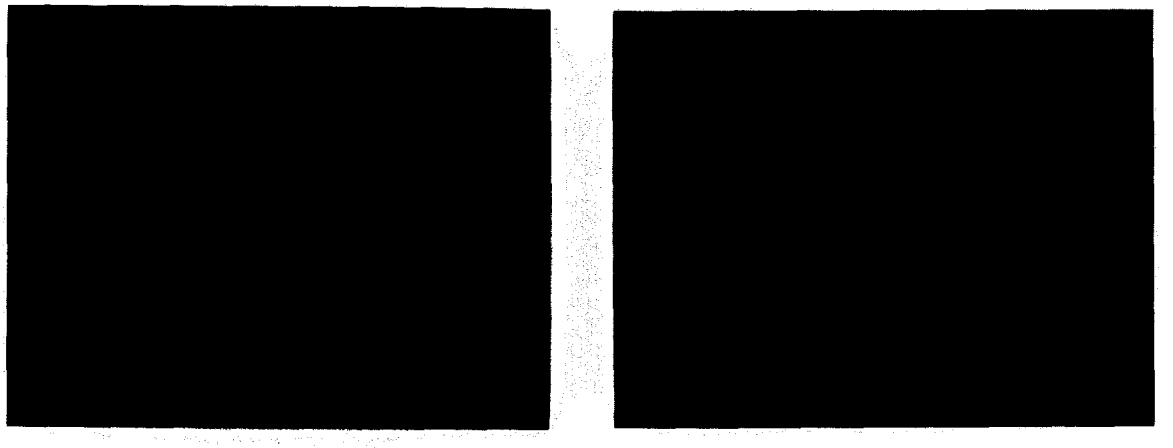

Fig. 15. Photomicrograph of a sample of the irregular-shaped particles (material A) taken from the part in direct contact with the wall, 1.5 cm below the piston. Magnification: (a) 125 ×; (b) 1250 ×.

that of virgin material. Samples 1 and, to a lesser degree, 4 contain a significant number of large aggregates. This is indicated by the small new mode observed with samples 1 and 4 in the range 50–120 μm. These aggregates of particles can also be seen in Figs. 14 and 15. They are formed during the consolidation of the packing and are incompletely redispersed during the treatment of the samples. Intense sonication prior to the determination of the size distribution was applied as a standard procedure to avoid counting agglomerates as individual particles. It might have been insufficient in this case, suggesting that the particles in these agglomerates stick strongly together. It is not to be excluded that the fusion of some particles, which is seen at high compression stress [6,7], has already begun to a moderate extent. Be that as it may, these agglomerates do not result in decreased column performance as long as they remain undisturbed in the column where they have been made.

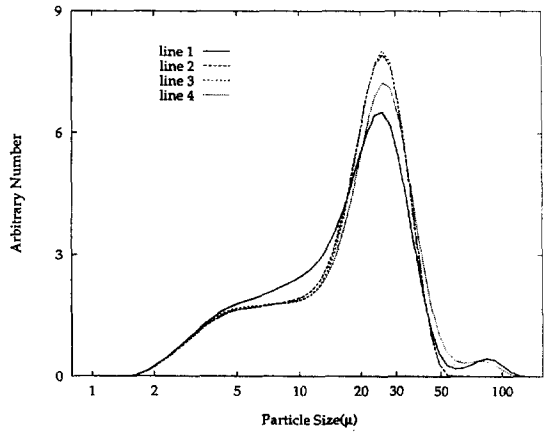

Fig. 16. Volume-based particle size distribution of samples of the irregular-shaped packing material A (abscissa, log d_p). Samples 1, 2: dry compression experiment; samples 3, 4: wet compression experiment [9]. Samples 1, 3: center of the packing, right against the piston frit; samples 2, 4: packing against the wall, at the bottom of the bed, close to the piston.

We do not know to which extent agglomeration affects the column performance. However, the fragmentation of the particles which has been reported above leads to significant problems. The most important seems to be a further reduction in the column permeability, which adds to the similar effect of the consolidation itself on the external porosity. However, the compression stresses applied here greatly exceed the value recommended by the manufacturer (35 to 50 kg/cm^2 for irregular-shaped particles, 65 to 100 kg/cm^2 for spherical ones). More importantly, the level of fragmentation observed at the level of compression stress conventionally used does not seem to cause any significant changes in the chromatographic behavior of this material. Columns prepared with irregular-shaped particle packing recycled from a previous column have performed as well as the original material [10].

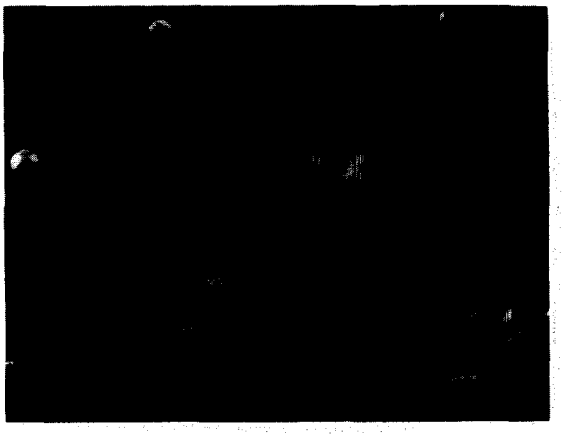

Fig. 17. Photomicrograph of the virgin spherical particles (material B). Magnification: 310 ×.

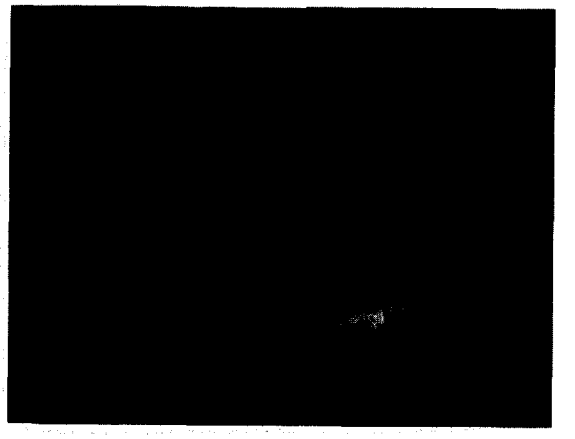

Fig. 18. Photomicrograph of a sample of the spherical particles (material B) taken from the part in direct contact with the piston frit, in the center of the column. Magnification: 1560 ×.

Spherical particles B

As illustrated in Fig. 17, the particles in the spherical material B are, in their vast majority, spherical in shape, with a diameter between 8 and 16 μm. A few anomalous particles were observed in some of the samples examined. They range from broken eggshells, to sphere agglomerates, to irregular-shaped particles. They seem to constitute fewer than 0.1% of the total number of particles. Because of their low number, their unusual shape, and their large size, these particles are more probably due to irregularities occurring during their production than to crushing during process, packaging and transportation. Few differences were found between photomicrographs obtained for samples of the virgin material B (Fig. 17) and of material collected at various places inside the bed, including locations close to the piston frit or to the column wall (Fig. 18), where the local stress is highest [6,7]. However, some small fragments are seen adhering to the larger spheres in Fig. 18. There are no similar particles in the virgin material (Fig. 17).

Significant but only small differences were observed for the volume statistics of the particle size distributions of the various samples. They are less important than for the irregular-shaped materials. Fig. 19 compares the particle size distribution of samples of the material B collected in the center of the packing, against the piston frit (sample 1) and against the wall, close to the piston (sample 2). In the former case, a few small agglomerates might have been formed. The extent of breakage appears to be negligible. As a matter of fact, the differences between the two distributions in Fig. 19 might well not be significant given the reproducibility of the measurements. We conclude that, although a maximum compression stress of 100 kg/cm^2 was applied to the bed from which the sample examined in Fig. 17 was taken, the extent of

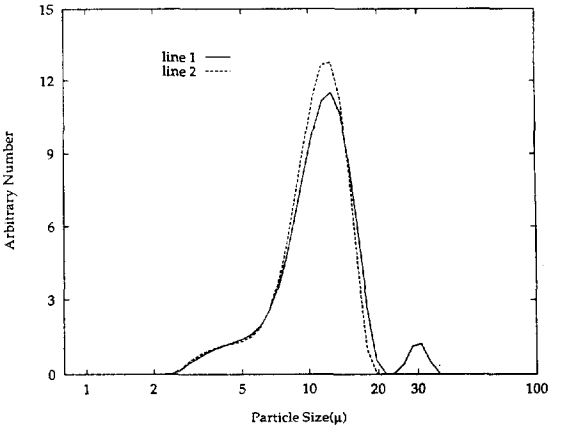

Fig. 19. Volume-based particle size distribution of samples of the spherical particles (material B). Sample 1: center of the packing, right against the piston frit; sample 2: packing against the wall, at the bottom of the bed, close to the piston.

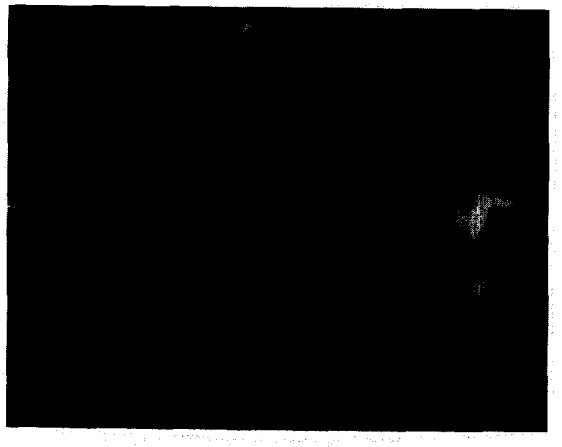

Fig. 20. Photomicrograph of the virgin spherical particles (material C). Magnification: 1250 × .

particle breakage observed with this spherical material is very limited.

Spherical particles C

Figs. 20 and 21 show typical photomicrographs made of a sample of the virgin material (Fig. 20) and of a sample of the same material (Fig. 21) taken from a region in contact with the wall and near the piston, after consolidation under high compression stress (94 kg/cm^2). This is the region where the stress is higher [6,7]. Both samples contain mostly spherical particles. There

Fig. 21. Photomicrograph of a sample of the spherical particles (material C) taken from the part in direct contact with the piston frit, along the column wall. Magnification: 1250 × .

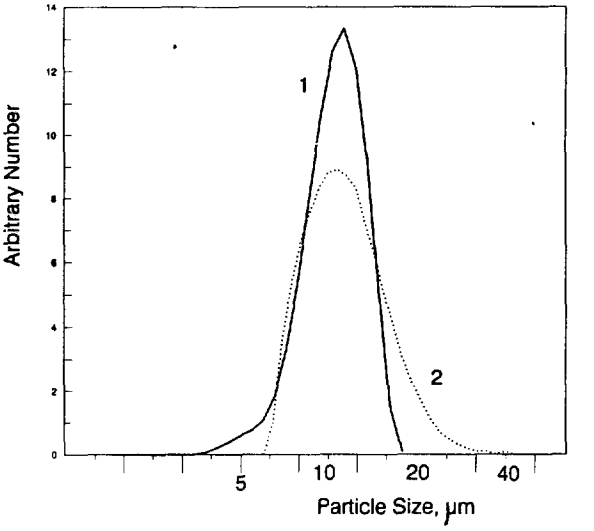

Fig. 22. Volume-based particle size distribution of samples of the spherical particles (material C). Sample 1: center of the packing, right against the piston frit; sample 2: packing against the wall, at the bottom of the bed, close to the piston.

appears to be about the same proportion of broken particles in the two samples. There are also a number of particles which are deformed, by partial fusion of several spheres or by dimples formed on their surface. However, there seem to be only very small differences between the two samples. A very small number of chip fragments can be seen in Fig. 21. The extent of fragmentation is negligible. Nevertheless, the existence of a significant fraction of nonspherical particles is the most probable explanation for the difference in the kinetics of consolidation of the materials B and C.

Finally, Fig. 22 compares the particle size distribution of a sample of the virgin material and a sample of material taken from the bed consolidated under 94 kg/cm^2. There is practically no difference between the volume based distribution of these samples. The extent of particle breakage is negligible under the experimental conditions of this study.

4. Conclusion

Beds of silica packing materials are compressible to a large degree, although their individual

particles are not. Thus, the packing density depends on the intensity of the compression stress applied. Whatever the nature of the particles, spherical or irregular, the length of the packing in an axial compression column decreases by approximately 25% when the compression stress is increased from a low value to a stress high enough to cause significant particle breakage. However, recompression of previously consolidated beds causes no further shrinkage.

Plots of column lengths versus time after a jump in the intensity of the compression stress applied and plots of column lengths after stabilization versus the intensity of the compression stress vary widely from material to material.

Acknowledgements

This work has been supported in part by Grant DE-FG05-88ER13859 of the US Department of Energy and by the cooperative agreement between the University of Tennessee and the Oak Ridge National Laboratory. We are grateful to J. Graue and E.L. Plowman (Mallinckrodt Chemical, St. Louis, MO, USA) and to Peter Cartier (Rohm and Haas, Spring House, PA, USA) who made the measurements to characterize the particles before and after compression, to Giorgio Carta (Department of Chemical Engineering, University of Virginia, Charlottesville, VA, USA) who brought the work of David Train to our attention, and to Luc Dormieux and Jean Salençon (Laboratoire de Mécanique des Solides, Ecole Polytechnique, Palaiseau, France) for fruitful discussions. We acknowledge the long term loan from Prochrom (Champigneulles, France) of the 5 cm I.D. stainless steel column and the axial compression unit. We thank Biotage (Charlottesville, VA, USA) for the long term loan of their Kiloprep 100 solvent delivery system and the Linear Scientific Model 204 UV detector equipped with a preparative scale cell. We thank BTR Separation, Wilmington, DE, USA (formerly The PQ Corporation) for their gift of a semipreparative Linear Scientific Detector and the companies which have given us the packing material used for this study.

References

[1] D.W. Taylor, Fundamentals of Soil Mechanics, Wiley, New York, 1948.
[2] K. Terzaghi, Erdbaumechanik, F. Deuticke, Vienna, Austria, 1925.
[3] K. Terzaghi, From Theory to Practice in Soil Mechanics, Wiley, New York, 1960.
[4] T.W. Lambe and R.V. Whitman, Soil Mechanics, Wiley, New York, 1969.
[5] C.E. Schwartz and J.M. Schmidt, Ind. Eng. Chem., 45 (1953) 1209.
[6] D. Train, J. Pharm. Pharmacol., 8 (1956) 745.
[7] D. Train, Trans. Inst. Chem. Eng., 35 (1957) 258.
[8] D. Train and J.A. Hearsey, J. Pharm. Pharmacol., 12 (1960) 97T.
[9] G. Guiochon and M. Sarker, J. Chromatogr. A, 704 (1995) 247.
[10] M. Sarker and G. Guiochon, J. Chromatogr. A, 702 (1995) 27.
[11] M. Sarker and G. Guiochon, J. Chromatogr. A, 709 (1995) 227.
[12] M. Sarker, T. Yun and G. Guiochon, in preparation.